Measurement of the Water Solubility in the Gas Phase of the Ethane + Water Binary System near Hydrate Forming Conditions

Antonin Chapoy, Christophe Coquelet, and Dominique Richon*

Centre d'Energétique, Ecole Nationale Supérieure des Mines de Paris CENERG/TEP, 35 Rue Saint Honoré, 77305 Fontainebleau, France

This project involves measurements of the vapor phase composition for the ethane + water binary system presenting phase equilibria near hydrate-forming conditions. The $H_2O + C_2H_6$ binary system isothermal vapor phase data, concerning both vapor−liquid and vapor−hydrate equilibria, were measured at (278.08, 283.11, 288.11, 293.11, 298.11, and 303.11) K and pressures up to the ethane vapor pressure. In this work a static−analytic apparatus, taking advantage of a pneumatic capillary sampler (Rolsi, Armines' patent) developed in the Cenerg/TEP laboratory, is combined with an exponential dilutor for calibration purposes and a *PVT* apparatus to visualize and determine the hydrate-forming conditions. The six sets of isothermal *P*, *y* data are represented with the Peng−Robinson equation of state (PR-EoS) using the Mathias−Copeman α function and the Huron−Vidal mixing rules involving the NRTL local composition model (PR-EoS/MC-HV-NRTL). This equation (PR-EoS/MC-HV-NRTL) is also used to fit the available literature data. A Henry's law approach was selected to treat the aqueous phase.

Introduction

Natural gas is rapidly growing in global importance both as an energy source and as a feedstock for downstream industry. When gas is produced offshore, the separation of liquid fractions and the removal of water are not carried out before the production flow is sent into pipelines. Consequently, water and light hydrocarbons are present; then for particular temperature and pressure conditions, hydrates can form during natural gas transport. Natural gas hydrates, also referred to as clathrates, are crystalline structures of water which surround low molecular weight gases, such as methane, ethane, propane, or butane. The hydrate crystals combine to form solid icelike crystals which can block production flow lines and tubing, causing shutdowns.

Accurate knowledge of water/hydrocarbon thermodynamic properties near the hydrate-forming conditions is of great interest to the petroleum industry. The purpose of this paper is to contribute to determining the behavior of some water/hydrocarbon binary systems near these conditions[1−4] (Figure 1).

At low temperatures the water content of natural gas is very low, and it is well-known that the measurement of water concentration in these gases is one of the most difficult problems of trace analysis. As a consequence, accurate water solubility measurements require special care. Therefore, the different isotherms presented herein were obtained using an apparatus based on a static−analytic method combined with a dilutor apparatus to calibrate the GC detector with water.

The experimental results were fitted using the Peng−Robinson equation of state (PR-EoS) using the Mathias-Copeman α function with the Huron−Vidal mixing rules involving the NRTL model. As the aqueous phase composition was not measured, it was estimated by means of a Henry's law approach using the determined vapor phase properties.

* Corresponding author. E-mail: richon@paris.ensmp.fr. Telephone: (33) 164694965. Fax (33) 164694968.

Experimental Section

Materials. Ethane was furnished by Messer Griesheim with a certified purity greater than 99.995 vol %. Helium from Air Liquide (France) is pure grade with traces of water (3 ppm) and of hydrocarbons (0.5 ppm). Helium was dried with molecular sieves.

Apparatus and Experimental Procedures. The apparatus used in this work (Figure 2) is based on a static−analytic method with vapor phase sampling. This apparatus is similar to that described by Laugier and Richon.[5]

The phase equilibrium is achieved in a cylindrical cell made of Hastelloy C276, the cell volume is about 34 cm^3 (internal diameter = 25 mm, height = 69.76 mm), and it can be operated up to 40 MPa between (223.15 and 473.15) K. The cell is immersed in an ULTRA-KRYOMAT LAUDA constant-temperature liquid bath that controls and maintains the desired temperature within ±0.01 K. To perform accurate temperature measurements in the equilibrium cell and to check for thermal gradients, temperature is measured at two locations corresponding to the vapor and liquid phase through two 100 Ω platinum resistance thermometer devices (Pt100) connected to an HP data acquisition unit (HP34970A). These two Pt100 are carefully and periodically calibrated against a 25 Ω reference platinum resistance thermometer (TINSLEY Precision Instruments). The resulting uncertainty is not higher than 0.02 K. The 25 Ω reference platinum resistance thermometer was calibrated by the Laboratoire National d'Essais (Paris) on the basis of the 1990 International Temperature Scale (ITS 90). Pressures are measured by means of two Druck pressure transducers (type PTX 610, range (0 to 30) MPa, and type PTX611, range (0 to 1.6) MPa) connected to the HP data acquisition unit (HP34970A); the pressure transducers are maintained at a constant temperature (temperature higher

10.1021/je0202230 CCC: $25.00
Published on Web 06/18/2003

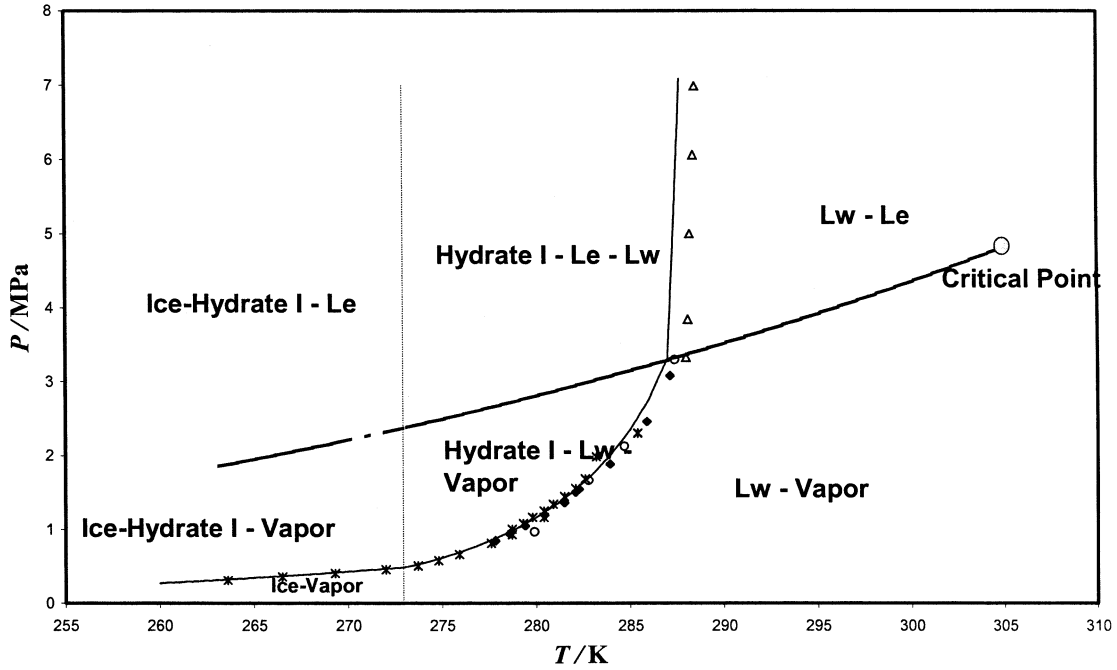

Figure 1. Pressure−temperature diagram for ethane and water: ∗, data from Deaton and Frost Jr.;[1] △, data from Ng and Robinson;[2] ○, data from Reamer et al.;[3] ♦, data from Holder et al.;[4] ···, ice vapor pressure; - - -, ethane vapor pressure; Lw, liquid water; Le, liquid ethane; |, calculated with the van der Waals and Platteuw model.[21]

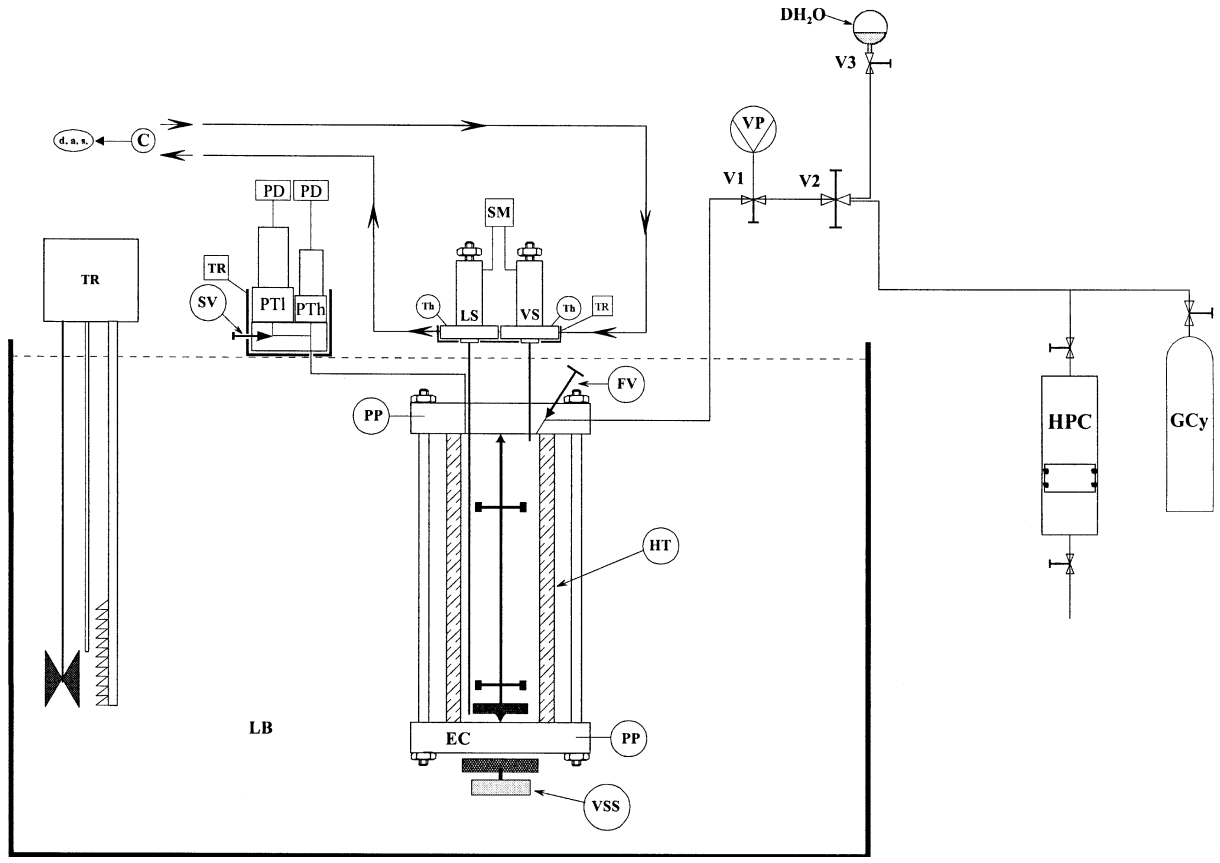

Figure 2. Flow diagram of the equipment: C, carrier gas; d.a.s., data acquisition system; DH_2O, degassed water; EC, equilibrium cell; FV, feeding valve; GCy, gas cylinder; HPC, high-pressure compressor; HT, Hastelstoy tube; LB, liquid bath; LS, liquid sampler; PP, platinum resistance thermometer probe; PT, pressure transducer; SM, sampler monitoring; SV, special valve; Th, thermocouple; TR, temperature regulator; V*i*, valve number *i*; VS, vapor sampler; VSS, variable speed stirrer; VP, vacuum pump.

than the highest temperature of the study) by means of a specially made air-thermostat, which is controlled using a PID regulator (WEST, model 6100). Both pressure transducers are calibrated against a dead weights pressure balance (Desgranges & Huot 5202S, CP (0.3 to 40) MPa, Aubervilliers, France). Pressure measurement uncertainties are estimated to be within ±0.5 kPa in the (0 to 2.5) MPa range using the (0 to 1.6) MPa pressure transducer and within ±5 kPa in the (2.5 to 38) MPa range using the (0 to 30) MPa pressure transducer.

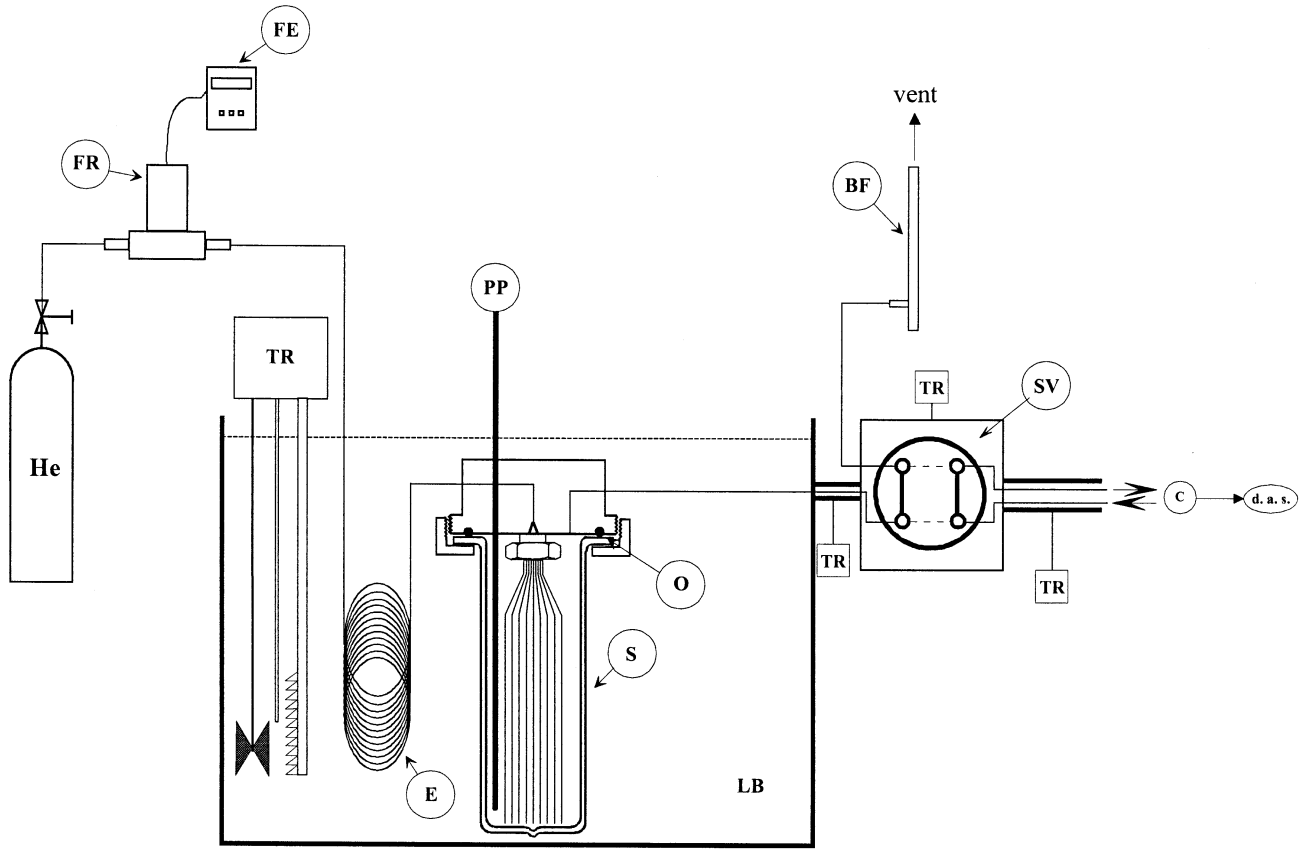

Figure 3. Flow diagram of the calibration circuit: BF, bubble flow meter; C, carrier gas; d.a.s., data acquisition system; E, heat exchanger; FE, flow rate electronic; FR, flow rate regulator; LB, liquid bath; O, O ring; PP, platinum resistance thermometer probe; S, saturator; SV, internal loop sampling valve; Th, thermocouple; TR, temperature regulator; VP, vacuum pump.

The HP on-line data acquisition unit is connected to a personal computer through an RS-232 interface. This system allows real time readings and storage of temperatures and pressures througout the different isothermal runs.

The analytical work was carried out using a gas chromatograph (VARIAN model CP-3800) equipped with two dectectors in series, a thermal conductivity detector (TCD) and a flame ionization detector (FID), connected to a data acquisition system (BORWIN ver 1.5, from JMBS, Le Fontanil, France). The analytical column is a Hayesep C 80/100 mesh column (silcosteel tube, length 2 m, diameter $^1/_8$ in.). The FID was used to detect ethane. It was repeatedly calibrated by introducing known amounts of ethane through a gas syringe in the injector of the gas chromatograph. The ethane calibration uncertainty is estimated to be within ±1%. As the water concentration is expected to be very low, calibrating the detectors is very difficult. It is indeed impossible to correctly inject the required small quantities in the chromatograph using syringes. In fact, the water quantity, which must be detected and quantified from solubility measurement samples, is of the same order as the water quantity adsorbed on the syringe needle walls (due to ambient humidity). For calibration purposes, a dilutor apparatus is used with a specific calibration circuit (Figure 3). Its equilibrium cell is immersed in a thermoregulated bath. Helium is bubbled through the water-containing equilibrium cell to be saturated, before entering the chromatograph through a (5 μL) internal loop injection valve. At given temperature and pressure in the equilibrium cell and volume of the loop injection valve, a well-defined amount of water can be injected into the chromatograph. The calculation of the amount of water is carried out using equilibrium and mass balance relationships. At thermodynamic equilibrium the fugacity of water is the same in both vapor and liquid phases and the water mole fraction remains constant when the saturated gas is heated in the internal loop valve, and is given by

$$f_w^L = f_w^V \tag{1}$$

with

$$f_w^L = f_w^{Lref}\,\gamma_w^L x_w \tag{2}$$

For a pressurized liquid,

$$f_w^{Lref} = f_w^{sat}\,\exp\left(\int_{P^{sat}}^{P}\left(\frac{v^L}{RT}\right)\mathrm{d}P\right) \tag{3}$$

Assuming the Poynting correction,

$$f_w^{Lref} = f_w^{sat}\,\exp\left(\left(\frac{v^L}{RT}\right)(P - P^{sat})\right) \tag{4}$$

equation 1 becomes

$$f_w^V = \gamma_w^L x_w f_w^{sat}\,\exp\left(\left(\frac{v^L}{RT}\right)(P - P^{sat})\right) \tag{5}$$

$$f_w^V = \gamma_w^L x_w P_w^{sat}\,\varphi_w^{sat}\,\exp\left(\left(\frac{v^L}{RT}\right)(P - P^{sat})\right) \tag{6}$$

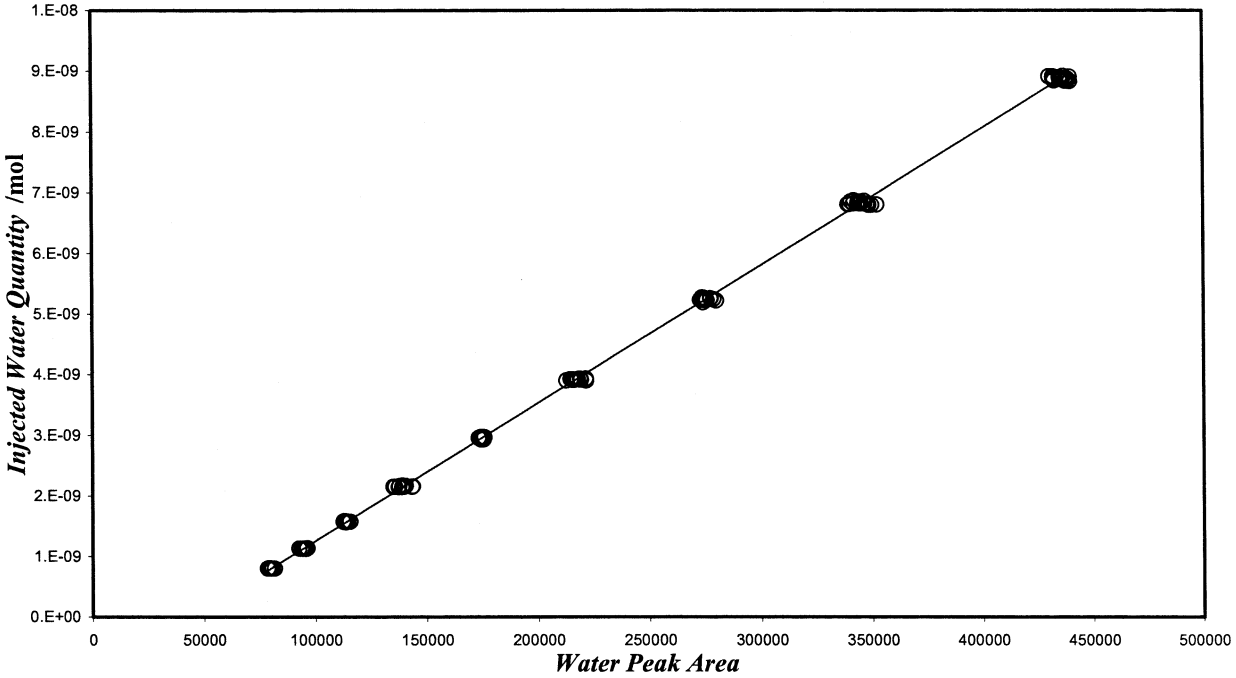

Figure 4. TCD calibration curve corresponding to water.

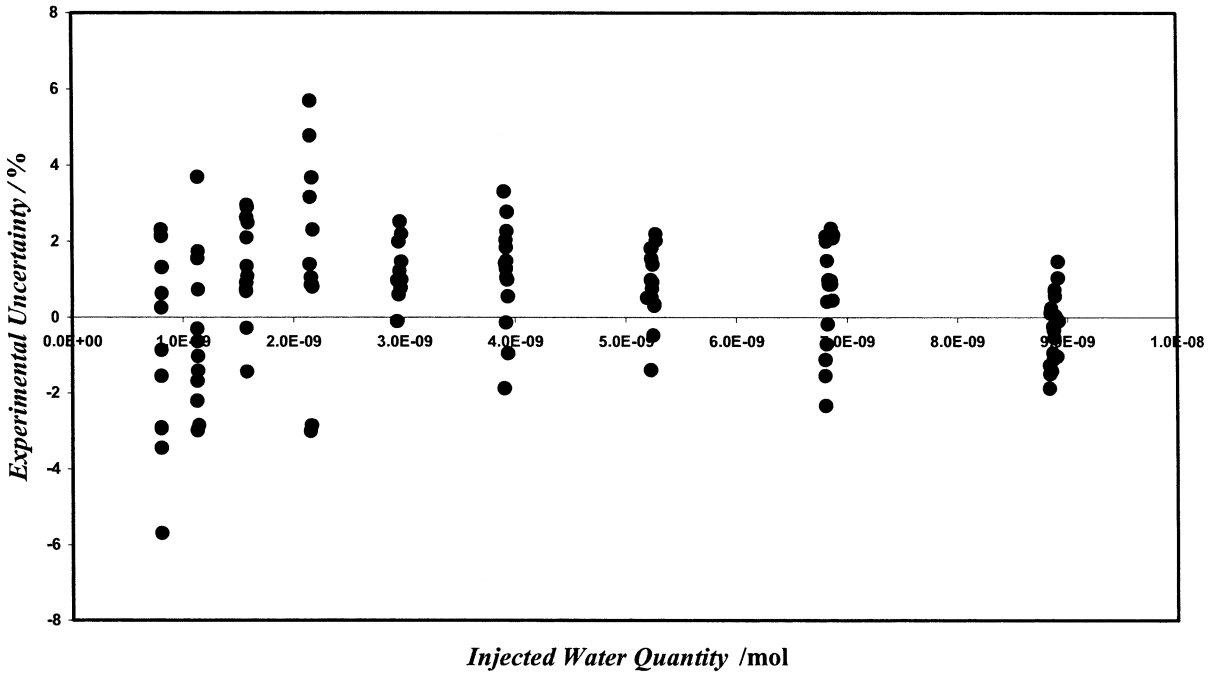

Figure 5. Water mole uncertainty through TCD analysis.

because

$$P_w^{sat}\,\varphi_w^{sat} = f_w^{sat} \tag{7}$$

On the other hand,

$$f_w^{V} = \varphi_w^{V} P_{dilutor} y_w \tag{8}$$

Thus,

$$y_w = \gamma_w^{L} x_w \frac{P_w^{sat}}{P_{dilutor}} \frac{\varphi_w^{sat}}{\varphi_w^{V}} \exp\left(\left(\frac{v^{L}}{RT}\right)(P - P^{sat})\right) \tag{9}$$

where

$$y_w = \frac{n_w}{n_T} \tag{10}$$

An exact relationship is obtained, given by

$$n_w = \gamma_w^{L} x_w \frac{P_w^{sat}}{P_{dilutor}} \frac{\varphi_w^{sat}}{\varphi_w^{V}} \left(\frac{PV}{ZRT}\right)^{loop} \exp\left(\left(\frac{v^{L}}{RT}\right)(P - P^{sat})\right) \tag{11}$$

Sources of numerical input for the equations above may be found in the section Aqueous Phase of the section Correlations.

Table 1. Critical Parameters and Acentric Factors

compound	P_c/MPa	T_c/K	ω
H_2O	22.05	647.13	0.3449
ethane	48.08	305.32	0.0995

To minimize the adsorption phenomenon, the internal injection valve was maintained at a high temperature, that is, 523.15 K. In the worst case the experimental uncertainty of the TCD water calibration (Figure 4, from (9×10^{-10} to 1.2×10^{-8}) mol) was estimated to not exceed ±6% (Figure 5).

Experimental Procedures. The equilibrium cell and its loading lines were evacuated down to 0.1 Pa, and the necessary quantity of the preliminary degassed water (approximately 10 cm^3) was introduced using an auxiliary cell. Then, the desired amount of ethane was introduced into the cell directly from the commercial cylinder or via a gas compressor.

For each equilibrium condition, at least 10 samples are withdrawn using the pneumatic samplers ROLSI[6] and analyzed in order to check for measurement repeatability. As the volume of the withdrawn samples is very small compared to the volume of the vapor phase present in the equilibrium cell, it is possible to withdraw many samples without disturbing the phase equilibrium.

Correlations

Vapor Phase. The critical temperature (T_C), critical pressure (P_C), and acentric factor (ω) for each of the two pure compounds are provided in Table 1. The experimental VLE data were correlated by means of in-house software, developed by Ecole des Mines de Paris. The Peng−Robinson[7] equation of state (PR-EoS) is selected because of its simplicity and its widespread utilization in chemical engineering. Moreover, this EoS gives better results for VLE of polar mixtures than the Soave−Redlich−Kwong[8] equation of state (SRK-EoS) and provides reliable calculations of the molar vapor volume. Its formulation is given by

$$P = \frac{RT}{v-b} - \frac{a(T)}{v(v+b)+b(v-b)} \tag{12}$$

where

$$b = 0.07780\frac{RT_C}{P_C} \tag{13}$$

and

$$a(T) = a_c\alpha(T_r) \tag{14}$$

where

$$a_C = 0.45724\frac{(RT_C)^2}{P_C} \tag{15}$$

To have an accurate representation of the vapor pressure of each component, the Mathias−Copeman α function,[9] especially developed for polar compounds, was selected,

$$\alpha(T) = \left[1 + c_1\left(1 - \sqrt{\frac{T}{T_C}}\right) + c_2\left(1 - \sqrt{\frac{T}{T_C}}\right)^2 + c_3\left(1 - \sqrt{\frac{T}{T_C}}\right)^3\right]^2 \tag{16}$$

Table 2. Correlation Coefficients for Ethane and Water (See Eq 29)

coefficient	ethane	H_2O
A/Pa	51.857	73.649
B/Pa·K	−2598.7	−7258.2
C/Pa·K^{-1}	−5.1283	−7.3037
D/Pa·K^{-E}	1.4913×10^{-5}	4.1653×10^{-6}
E	2	2

Table 3. Calculated Pressures P_e (from the Correlation in Eq 29) along with Calculated Pressures $P_{e,cal}$ from the PR-EoS Using the Mathias−Copeman α Function

T/K	P_w/Pa	$P_{w,cal}$/Pa	P_e/MPa	$P_{e,cal}$/MPa
273.15	610	610	2.39	2.40
278.15	872	872	2.69	2.70
283.15	1227	1228	3.02	3.04
288.15	1705	1705	3.38	3.40
293.15	2339	2339	3.77	3.79
298.15	3170	3171	4.19	4.21
303.15	4248	4248	4.64	4.67

If $T > T_C$,

$$\alpha(T) = \left[1 + c_1\left(1 - \sqrt{\frac{T}{T_C}}\right)\right]^2 \tag{17}$$

c_1, c_2, and c_3 are adjustable parameters that were evaluated for our whole temperature domain using a modified Simplex algorithm.[10] The objective function is

$$F_P = \frac{100}{N}\sum_{i=1}^{N}\left(\frac{P_{i,exp} - P_{i,cal}}{P_{i,exp}}\right)^2 \tag{18}$$

where N is the number of data points, P_{exp} is the measured pressure, and P_{cal} is the calculated pressure.

The infinite pressure reference Huron−Vidal mixing rules[11] where the attractive parameter, a, is calculatedfrom eq 19 and the molar covolume, b, is calculated from eq 20 are

$$a = b\left(\sum_i x_i\left(\frac{a_i}{b_i}\right) + G^E_{P=\infty}C\right) \tag{19}$$

$$b = \sum_i x_i b_i \tag{20}$$

$$C = \ln\left(\frac{1}{2}\right) \tag{21}$$

The excess Gibbs energy is calculated using the NRTL[12] local composition model.

$$\frac{G^E_{(T,P)}}{RT} = \sum_i x_i \sum_j \frac{x_j \exp\left(-\alpha_{j,i}\frac{\tau_{j,i}}{RT}\right)}{\sum_k x_k \exp\left(-\alpha_{k,i}\frac{\tau_{k,i}}{RT}\right)}\tau_{j,i} \tag{22}$$

where $\tau_{i,i} = 0$ and $\alpha_{i,i} = 0$, and $\alpha_{j,i}$, $\tau_{j,i}$, and $\tau_{i,j}$ are adjustable parameters. For this system, which belongs to a given polar mixture type, it is recommended[9] to use $\alpha_{j,i} = 0.3$. Then only $\tau_{j,i}$ and $\tau_{i,j}$ are adjusted directly to VLE data through a modified Simplex algorithm using the objective function,

Table 4. Water Mole Fraction in the Gas Phase of the Ethane + Water System

T/K	P_{exp}/MPa	$10^3 y_{w,exp}$	$10^3 y_{w,cal}$(HV)	Dy/%
278.08	0.455	2.05	2.11	−2.72
278.08	0.756	1.27	1.26	0.96
278.08	0.99	0.898	0.907	−1.05
278.08	1.23	0.673	0.662	1.7
278.08	1.51	0.476	0.474	0.3
278.08	1.58	0.453	0.438	3.50
278.08	2.11	0.304	0.326	−6.68
278.08	2.71	0.215	0.215	0.00
283.11	0.323	4.21	3.92	7.46
283.11	0.388	3.51	3.32	5.90
283.11	0.415	3.28	3.13	4.71
283.11	0.621	2.12	2.23	−5.06
283.11	0.774	1.71	1.78	−4.16
283.11	0.962	1.34	1.41	−4.90
283.11	1.05	1.17	1.26	−7.72
283.11	1.45	0.816	0.812	0.43
283.11	1.82	0.575	0.568	1.18
283.11	2.11	0.501	0.507	−1.16
283.11	2.35	0.436	0.440	−0.89
283.11	2.78	0.352	0.343	2.56
283.11	2.99	0.304	0.302	0.78
288.11	0.898	2.32	2.21	5.28
288.11	1.39	1.41	1.41	0.36
288.11	1.91	0.934	0.956	−2.26
288.11	2.49	0.644	0.663	−2.80
288.11	2.85	0.541	0.550	−1.64
288.11	3.19	0.461	0.461	0.00
288.11	3.36	0.427	0.422	1.20
293.11	0.401	6.79	7.01	−3.11
293.11	0.527	5.20	5.14	1.08
293.11	0.774	3.48	3.35	3.74
293.11	1.22	2.06	2.05	0.61
293.11	1.5	1.67	1.78	−6.48
293.11	2.56	0.895	0.883	1.41
293.11	3.24	0.660	0.660	−0.03
293.11	3.32	0.626	0.638	−1.87
293.11	3.48	0.595	0.595	0.00
293.11	3.75	0.525	0.523	0.37
298.11	1.08	3.86	3.56	8.34
298.11	1.43	2.85	2.65	7.80
298.11	2.19	1.78	1.68	5.55
298.11	2.73	1.37	1.30	5.57
298.11	3.53	0.982	0.940	4.51
298.11	3.99	0.794	0.794	0.00
298.11	4.01	0.768	0.788	−2.49
298.11	4.12	0.749	0.755	−0.79
303.11	0.649	8.54	7.69	11.12
303.11	0.966	5.74	5.17	11.08
303.11	1.76	3.07	2.89	5.98
303.11	2.48	1.98	1.98	0.00
303.11	3.37	1.41	1.38	2.41
303.11	4.38	0.990	0.990	0.00
303.11	4.48	0.943	0.957	−1.40
303.11	4.63	0.911	0.901	1.09

displayed in eq 18,

$$F_y = \frac{100}{N}\sum_{1}^{N}\left(\frac{y_{i,\mathrm{exp}} - y_{i,\mathrm{cal}}}{y_{i,\mathrm{exp}}}\right)^2 \qquad (23)$$

where N is the number of data points, y_{exp} is the measured pressure, and y_{cal} is the calculated pressure.

Aqueous Phase. At the thermodynamic equilibrium the fugacity, f_e, of ethane is the same in both vapor and liquid phases.

$$f_e^{L}(P,T) = f_e^{V}(P,T) \qquad (24)$$

The vapor fugacity is calculated with

$$f_e^{V}(P,T) = \varphi_e^{V} P y_e \qquad (25)$$

However, the fugacity coefficient in the vapor phase is calculated as a first approximation using the fugacity of pure ethane. For the aqueous phase, a Henry's law approach is used for both compounds. As ethane is infinitely diluted in water, the dissymmetric convention ($\gamma_e \rightarrow 1$ when $x_e \rightarrow 0$) is used to express the law for the hydrocarbon (eq 26) while a symmetric convention ($\gamma_w \rightarrow 1$ when $x_w \rightarrow 1$) is used for water (eq 27)

Table 5. Values of the Adjusted Mixing Rules' Parameters and of the Objective Function at Each Temperature

T/K	τ_{12}/J·mol^{-1}	τ_{21}/J·mol^{-1}	F
278.08	23 408	34 414	1.8
283.11	23 949	31 335	4.08
288.11	25 182	24 495	1.7
293.11	23 778	26 865	2.52
298.11	26 521	22 633	4.13
303.11	28 218	22 258	3.8

Table 6. Bias(y) and MRD(y), Using the Peng−Robinson Equation of State with Huron−Vidal Mixing Rules

T/K	Bias(y)$_{HV}$/%	MRD(y)$_{HV}$/%
283.08	6.19	0.38
288.11	5.47	−0.47
293.11	4.95	−4.60
298.11	4.86	−0.59
303.11	2.02	1.37
308.11	2.64	0.71
313.12	3.40	1.23
318.12	4.80	0.84

Table 7. Calculated Water Mole Fraction in the Aqueous Phase

P/MPa	$10^5 y_{e,cal}$	P/MPa	$10^5 y_{e,cal}$
	T/K = 278.08		
0.300	19	0.600	36
0.400	24	0.700	41
0.455	28	0.756	44
0.500	30		
	T/K = 283.11		
0.323	17	0.962	46
0.388	20	1.05	49
0.415	21	1.45	65
0.621	31	1.82	77
0.774	38		
	T/K = 288.11		
0.50	21	1.91	68
0.60	25	2.49	83
0.70	29	2.85	90
0.80	33	3.19	97
0.90	36	3.36	99
1.39	53		
	T/K = 293.11		
0.401	15	2.56	73
0.527	19	3.24	85
0.774	27	3.32	86
1.22	41	3.48	89
1.50	49	3.75	92
	T/K = 298.11		
1.08	32	3.53	79
1.43	41	3.99	84
2.19	58	4.01	84
2.73	68	4.12	86
	T/K = 303.11		
0.65	18	3.37	69
0.97	26	4.38	79
1.76	43	4.48	80
2.48	56	4.63	81

$$f_e^{L}(P,T) = H_w^{L}(T)\, x_e(T) \exp\left(\left(\frac{v_e^{\infty}(T)}{RT}\right)(P - P_w^{sat})\right) \qquad (26)$$

$$f_w^{L}(P,T) = \gamma_w^{L}\varphi_w^{sat} P_w^{sat} x_w(T) \exp\left(\left(\frac{v_w^{sat}(T)}{RT}\right)(P - P_w^{sat})\right) \qquad (27)$$

$$x_e(T) = \frac{P\varphi_e^{V} y_e(T)}{H_w^{L}(T) \exp\left(\left(\frac{v_e^{\infty}(T)}{RT}\right)(P - P_w^{sat})\right)} \qquad (28)$$

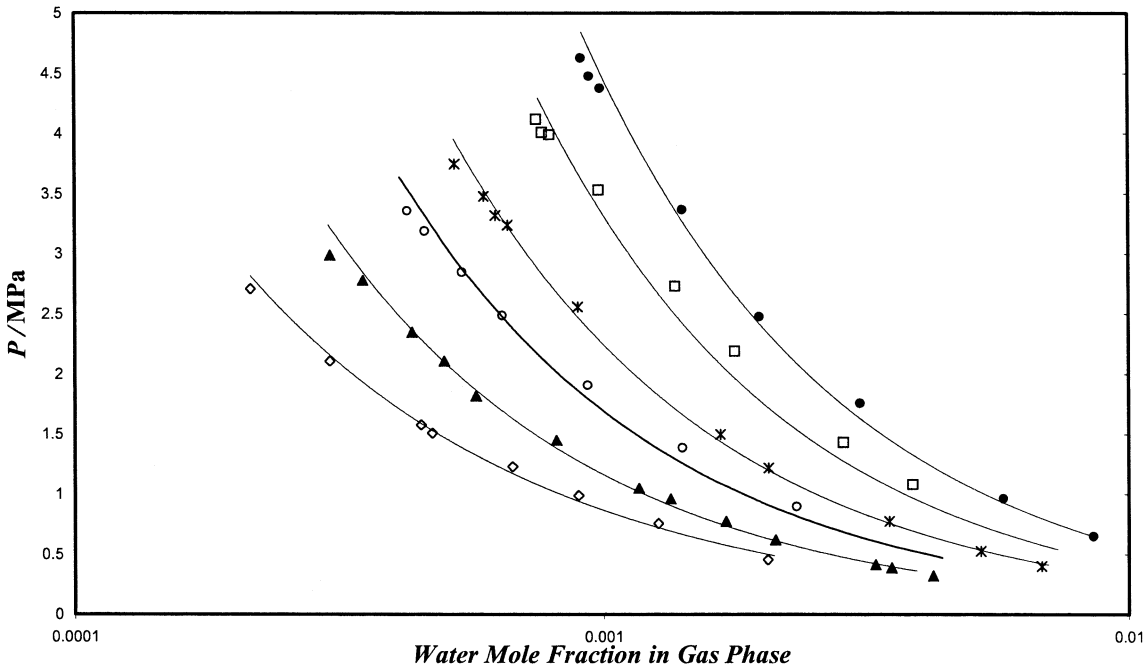

Figure 6. Pressure as a function of water mole fraction at different temperatures (semilogarithmic scale): ◇, 278.08 K; ▲, 283.11 K; ○, 288.11 K; ∗, 293.11 K; □, 298.11 K; ●, 303.11 K; solid lines, calculated with the PR-EoS, Huron−Vidal mixing rules, and the NRTL activity coefficient model with parameters from Table 10.

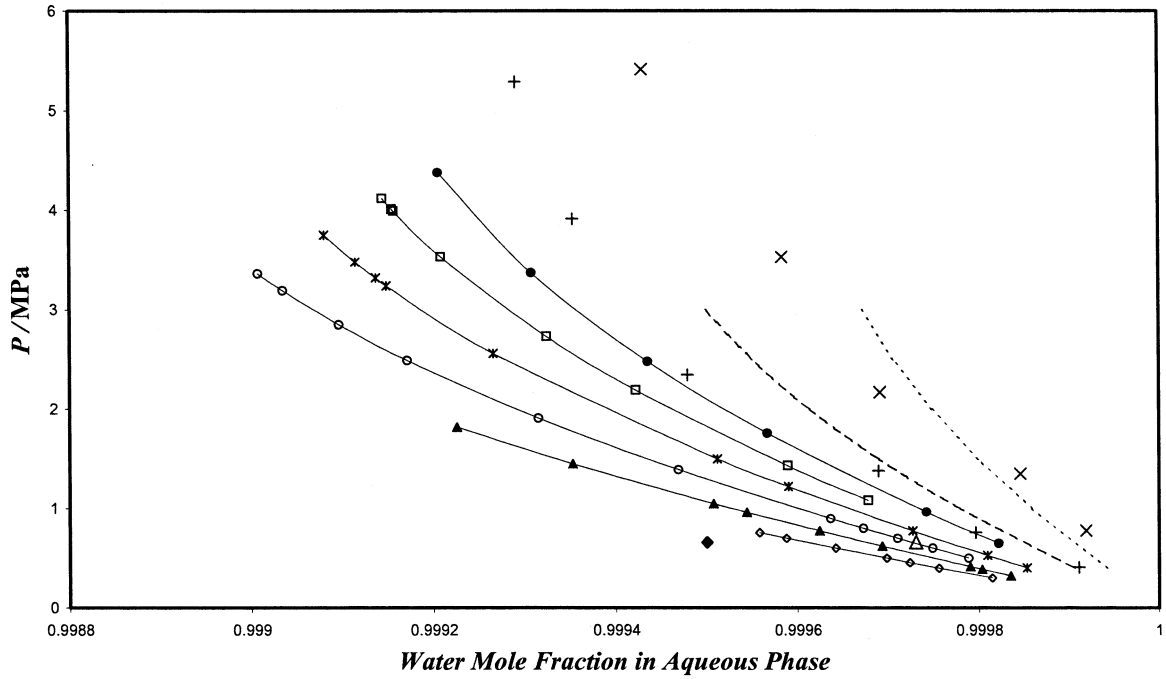

Figure 7. Pressure as a function of calculated water mole fraction in the aqueous phase at different temperatures: ◇, 278.08 K; ▲, 283.11 K; ○, 288.11 K; ∗, 293.11 K; □, 298.11 K; ●, 303.11 K; △, data of Song et al.[20] at 288.15 K; ■, data of Song et al.[20] at 283.15 K; +, data of Culberson and Mc Ketta[19] at 310.15 K; ×, data of Culberson and Mc Ketta[19] at 344.59 K.

The vapor pressures of water are calculated using the correlation in eq 29.[13]

$$P^{sat}(T) = e^{(A+(B/T)+C\ln(T)+DT^E)} \quad (29)$$

where A, B, C, D, and E are the coefficients reported in Table 2.

The partial molar volume of ethane at infinite dilution and 298.15 K is based on the work of Kobayashi and Katz;[14] its value is 0.053 $m^3 \cdot kmol^{-1}$ at atmospheric pressure. For temperature dependence, the following classical correction[14] is used:

$$v_e^{\infty}(T) = v_e^{\infty}(298.15K)\, v_e^{sat}(T)/v_e^{sat}(298.15K) \quad (30)$$

The Henry's law constants for ethane come from the literature[15] and are fitted using the correlation

$$\log_{10}(H_{ew}(T)) = 108.9263 - 5.51363 \times 10^3/T - 3.17413 \times 10^1 \log_{10}(T) \quad (31)$$

where H_{ew} is in atmospheres.

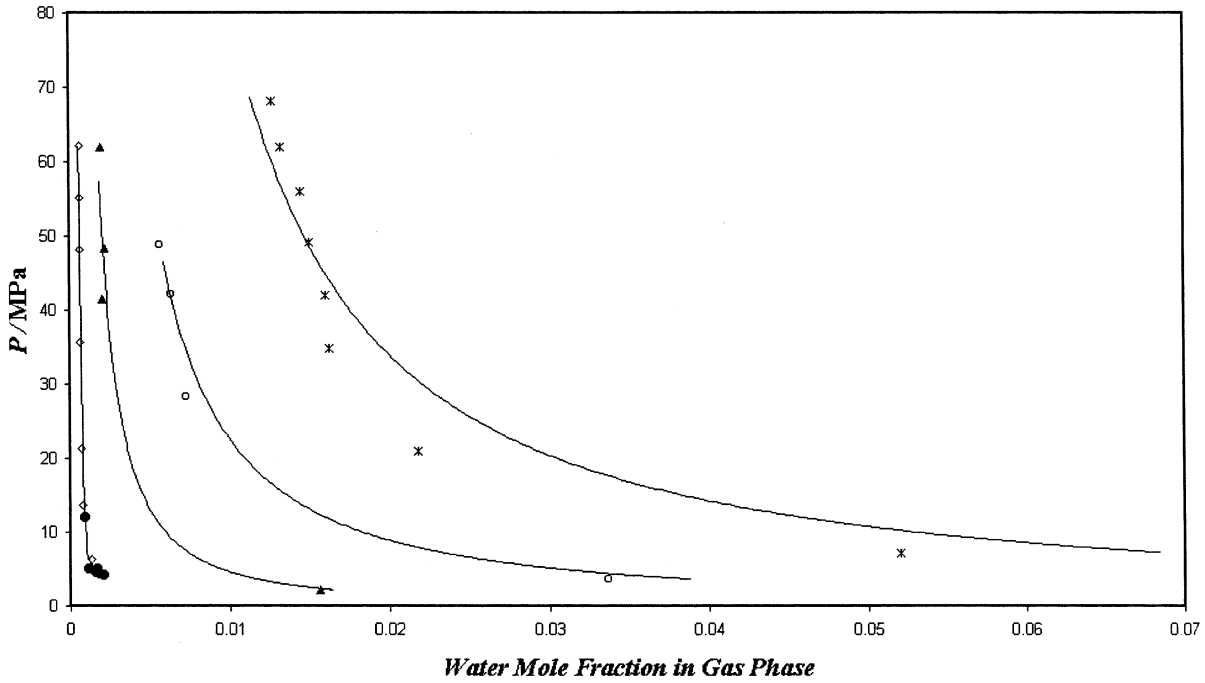

Figure 8. Pressure as a function of water mole fraction at different temperatures (semilogarithmic scale): ◇, Reamer et al.[17] at 310.93 K; ▲, Reamer et al.[17] at 344.26 K; ○, Reamer et al.[17] at 377.59 K; ∗, Reamer et al.[17] at 410.93 K; ●, data of Culberson and Mc Ketta[16] at 310.93 K; solid lines, calculated with the PR-EoS, Huron−Vidal mixing rules, and the NRTL activity coefficient model with parameters from Table 10.

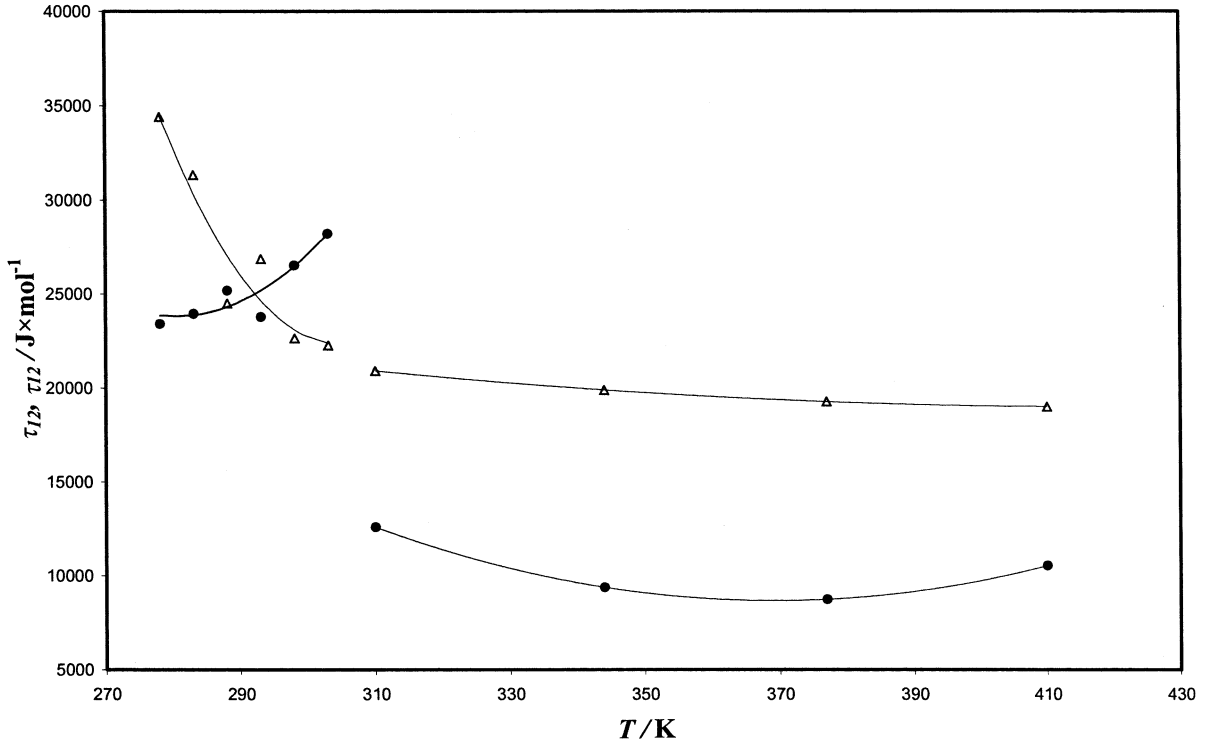

Figure 9. τ_{12} and τ_{21} NRTL binary parameters as a function of temperature: △, τ_{12}; ●, τ_{21}. Values are adjusted at each temperature independently. Solid line: binary parameters from eqs 34 and 35.

The above correlation is valid only for the temperature range from (275.15 to 323.15) K.

Results

Vapor Pressures. In this work, water and ethane vapor pressures are calculated using the correlation defined by eq 29 and then used to adjust the parameters of the Mathias−Copeman α function in the PR-EoS. After parameter adjustment, it is possible to generate a new set of water and ethane vapor pressures that are directly compared to the correlation values (Table 3). Deviations between the two data sets are less than 0.55%.

Vapor−Liquid and Vapor−Hydrate Equilibria. The VLE experimental and calculated data are reported in Table 4 and plotted in Figure 6. The parameters adjusted and the values of the objective function corresponding to

the PR-EoS + HV mixing rules and NRTL model are given in Table 5.

The deviations MRD(y) of vapor phase mole fractions, as defined by eq 32, are listed in Table 6; N is the number of data points

$$\mathrm{MRD}(y) = (100/N)\sum[|(y_{i,\mathrm{cal}} - y_{i,\mathrm{exp}})/y_{i,\mathrm{exp}}|] \quad (32)$$

The Bias values are also calculated and listed in Table 6 for all the cases,

$$\mathrm{Bias}(y) = (100/N)\sum((y_{i,\mathrm{exp}} - y_{i,\mathrm{cal}})/y_{i,\mathrm{exp}}) \quad (33)$$

All the data are well represented by this adjustment at each temperature.

Below the hydrate-forming conditions, the mole fraction of water in the aqueous phase was calculated with the model involving the Henry's law approach. The calculated data are reported in Table 7 and plotted in Figure 7.

Discussion

Our isothermal P, y data sets are well represented with the Peng−Robinson equation of state using the Mathias−Copeman α function and the Huron−Vidal mixing rules involving the NRTL model (deviations generally less than ±5%). As a validation of this model, data sets from Culberson and Mc Ketta[16] and Reamer et al.[17] have been fitted from (310.93 up to 410.93) K (Figure 8). Huron−Vidal mixing rules' binary interaction parameters (τ_{12}, τ_{21}) were calculated at each temperature; they are plotted in Figure 9 as a function of temperature from (283.08 to 303.11) K. The binary parameters have been adjusted on all data (all isotherms) assuming a second-order temperature dependence (eqs 34 and 35).

$$\tau_{12}(T) = \begin{cases} 8.42913T^2 - 4725.628T + 686001 \text{ if } T < T_C \\ 0.168T^2 - 139.710T + 48124 \text{ if } T > T_C \end{cases} \quad (34)$$

$$\tau_{21}(T) = \begin{cases} 17.00958T^2 - 10368.475T + 1602408 \text{ if } T < T_C \\ 1.122T^2 - 828.420T + 161590 \text{ if } T > T_C \end{cases} \quad (35)$$

The corresponding curves are plotted in Figure 9 along with binary parameter values adjusted at each temperature.

Binary interaction parameters (τ_{12}, τ_{21}) exhibit behaviors that are different below and above the ethane critical temperature. This phenomenon observed in Figure 9 is explained by the fact that properties of a supercritical gas in a liquid differ from those of a subcritical gas.[18] It is highly possible that new interactions are generated leading to a significant jump in the binary interaction parameter values.

Using the adjusted water mole fraction in the gas phase with the data set of Reamer et al.[17] at (310.93 and 344.26) K, the solubility calculations of the water distribution in the aqueous phase of the system have been carried out with the Henry's law approach and compared with data from Culberson and McKetta[19] at both temperatures (Figure 7). The calculated water mole fractions in the aqueous phase display a good agreement with the data sets below 3 MPa.

The experimental solubility measurements of the ethane distribution in the aqueous phase of the ethane + water binary system of Song et al.[20] tend to disagree at decreasing temperatures (Figure 7). At temperatures below 283 K, the solubility of ethane cannot be described using a Henry's law approach. There is a strong deviation between the experimental data set of these authors and the result given by the Henry's law approach. Song et al.[20] suggest "the onset of the sorption effect that will increase the solubility by almost two to three factors of magnitude will cause divergence of the Henry's law behavior". Therefore, below the hydrate-forming conditions, a Henry's law prediction cannot be used in its simple form to predict the solubility in the aqueous phase. At temperatures higher than 283 K, the solubility calculations of the water distribution in the aqueous phase of the system using the Henry's law approach are in good agreement with the data from Song et al.[20]

Conclusion

This paper presents solubility measurements of the water distribution in the vapor phase of the ethane + water mixture near hydrate-forming conditions. A static−analytic method to obtain the experimental data was used. The Peng−Robinson (PR) equation of state with the Mathias−Copeman α function was chosen to fit these data with HV mixing rules. Generally, the data are found to be consistent with the models. A simple model, taking advantage of a Henry's law approach, has been exposed to calculate the solubility of ethane in water. This simple approach is no more consistent near the hydrate-forming conditions, but it gives good results in VLE conditions.

List of Symbols

a = parameter of the equation of state (energy parameter Pa·m^6·mol^{-2})
b = parameter of the equation of state (covolume parameter m^3·mol^{-1})
G = Gibbs energy
C = numerical constant = ln(1/2)
F = objective function
P = pressure (MPa)
R = gas constant (J·mol^{-1}·K^{-1})
T = temperature (K)
Z = compressibility factor
x = liquid mole fraction
y = vapor mole fraction
D = relative deviation [DU = ($U_{\mathrm{exp}} - U_{\mathrm{cal}}$)/$U_{\mathrm{exp}}$]

Greek Letters

α_{ij} = NRTL model parameter (eq 11)
τ_{ij} = NRTL model binary interaction parameter (eq 11) (J·mol^{-1})
ω = acentric factor
Δ = deviation ($\Delta U = U_{\mathrm{exp}} - U_{\mathrm{cal}}$)

Superscripts

E = excess property
ref = reference property
L = liquid state
V = vapor state
sat = property at saturation
∞ = infinite dilution

Subscripts

C = critical property
cal = calculated property
exp = experimental property
i, j = molecular species
∞ = infinite pressure reference state
w or (1) = water

e or (2) = ethane
T = total

Literature Cited

(1) Deaton, W. M.; Frost, E. M., Jr. Gas Hydrates and their Relation to the Operation of Natural Gas Pipelines. *US Bureau of Mines Monograph 8*; 1946.

(2) Ng, H.-J.; Robinson, D. B. Hydrate Formation in Systems Containing Methane, Ethane, Propane, Carbon Dioxide or Hydrogen Sulfide in the Presence of Methanol. *Fluid Phase Equilib.* **1985**, *21*, 145−155.

(3) Reamer, H. H.; Selleck, F. T.; Sage, B. H. Some Properties of Mixed Paraffinic and Olefinic Hydrates. *J. Pet. Technol.* **1952**, *4*, 197−202.

(4) Holder, G. D.; Hand, J. H. Multiple-Phase Equilibria in Hydrates from Methane, Ethane, Propane and Water Mixtures. *AIChE J.* **1982**, *28*, 440−447.

(5) Laugier, S.; Richon, D. New Apparatus to perform fast Determinations of Mixture Vapor − Liquid Equilibria up to 10 MPa and 423 K. *Rev. Sci. Instrum.* **1986**, *57*, 469−472.

(6) Guilbot, P.; Valtz, A.; Legendre, H.; Richon, D. Rapid On-Line Sampler Injector. *Analusis* **2000**, *28*, 426−431.

(7) Peng, D. Y.; Robinson, D. B. A New two Constant Equation of State. *Ind. Eng. Chem. Fundam.* **1976**, *15*, 59−64.

(8) Soave, G. Equilibrium Constants for Modified Redlich-Kwong Equation of State. *Chem. Eng. Sci.* **1972**, *4*, 1197−1203.

(9) Mathias, P. M.; Copeman, T. W. Extension of the Peng−Robinson Equation of State to Complex Mixtures: Evaluation of the Various Forms of the Local Composition Concept. *Fluid Phase Equilib.* **1983**, *13*, 91−108.

(10) Renon, H.; Prausnitz, J. M. Local Compositions in Thermodynamic Excess Function for Liquid Mixtures. *AIChE J.* **1968**, *14*, 135−144.

(11) Huron, J. M.; Vidal, J. New Mixing Rules in Simple Equations of State for Representing Vapor-Liquid Equilibria of Strongly Non-Ideal Mixture. *Fluid Phase Equilib.* **1979**, *3*, 255−271.

(12) Åberg, E. R.; Gustavsson, A. G. Design and Evaluation of Modified Simplex Methods. *Anal. Chim. Acta* **1982**, *144*, 39−53.

(13) Reid, R. C.; Prauznitz, J. M.; Poling, B. E. *The Properties of Gases and Liquids*, 4th ed.; McGraw-Hill: New York, 1988.

(14) Kobayashi, R.; Katz, D. L. Vapor-Liquid Equilibria for Binary Hydrocarbon−Water Systems. *J. Eng. Chem.* **1953**, *45*, 450−451.

(15) Yaws, C. L.; Hopper, J. R.; Wang, X.; Rathinsamy, A. K.; Pike, R. W. Calculating Solubility & Henry's Law Constants for Gases in Water. *Chem. Eng.* **1999**, *June*, 102−105.

(16) Culberson, O. L.; McKetta, J. J., Jr. Phase Equilibria in Hydrocarbon−Water Systems IV− Vapor-Liquid Equilibrium Constants in the Methane-Water and Ethane-Water Systems. *Trans. Am. Inst. Min., Metall. Pet. Eng.* **1951**, *192*, 297−300.

(17) Reamer, H. H.; Olds, R. H.; Sage, B. H.; Lacey, W. N. Phase Equilibria in Hydrocarbon Systems. *Ind. Eng. Chem.* **1942**, *35*, 790−793.

(18) Valtz, A.; Coquelet, C.; Baba-Ahmed, A.; Richon, D. Vapor − Liquid Equilibrium Data for the CO_2 + 1,1,1,2,3,3,3-Heptafluoropropane (R227ea) System at Temperatures from 276.01 to 367.30 K and Pressures up to 7.4 MPa. *Fluid Phase Equilib.* **2003**, *207*, 53−67.

(19) Culberson, O. L.; McKetta, J. J., Jr. Phase Equilibria in Hydrocarbon−Water Systems: the solubility of Ethane in Water at Pressures up to 1200 Pounds per Square Inch. *Trans. Am. Inst. Min., Metall. Pet. Eng.* **1950**, *189*, 1−6.

(20) Song, K. Y.; Fneyrou, G.; Martin, R.; Lievois, J.; Kobayashi, R. Solubility Measurements of Methane and Ethane in Water and near Hydrate Conditions. *Fluid Phase Equilib.* **1997**, *128*, 249−260.

(21) Van der Waals, J. H.; Platteeuw, J. C. Clathrate Solutions. *Adv. Chem. Phys.* **1959**, *2*, 2−57.

Received for review December 17, 2002. Accepted May 7, 2003.

JE0202230